A Comprehensive Metabolomic Investigation in Urine of Mice Exposed to Strontium-90

Author(s): Maryam Goudarzi, Waylon M. Weber, Tytus D. Mak, Juijung Chung, Melanie Doyle-Eisele, Dunstana R. Melo, Steven J. Strawn, David J. Brenner, Raymond A. Guilmette and Albert J. Fornace, Jr.
Source: Radiation Research, 183(6):665-674.
Published By: Radiation Research Society
DOI: http://dx.doi.org/10.1667/RR14011.1
URL: http://www.bioone.org/doi/full/10.1667/RR14011.1

RADIATION RESEARCH **183**, 665–674 (2015)
0033-7587/15 $15.00

DOI: 10.1667/RR14011.1

A Comprehensive Metabolomic Investigation in Urine of Mice Exposed to Strontium-90

Maryam Goudarzi,[a,1] Waylon M. Weber,[b] Tytus D. Mak,[c] Juijung Chung,[a] Melanie Doyle-Eisele,[b] Dunstana R. Melo,[b] Steven J. Strawn,[a] David J. Brenner,[d] Raymond A. Guilmette[b] and Albert J. Fornace, Jr.[a,c]

[a] *Biochemistry and Molecular and Cellular Biology, Georgetown University, Washington D.C.;* [b] *Lovelace Respiratory Research Institute, Albuquerque, New Mexico;* [c] *Mass Spectrometry Data Center, National Institute of Standards and Technology, Gaithersburg, Maryland; and* [d] *Center for Radiological Research, Columbia University, New York, New York*

Goudarzi, M., Weber, W. M., Mak, T. D., Chung, J., Doyle-Eisele, M., Melo, D. R., Strawn, S. J., Brenner, D. J., Guilmette, R. A. and Fornace, Jr., A. J. A Comprehensive Metabolomic Investigation in Urine of Mice Exposed to Strontium-90. *Radiat. Res.* 183, 665–674 (2015).

Internal emitters such as Strontium-90 (^{90}Sr) pose a substantial health risk during and immediately after a nuclear disaster or detonation of an improvised device. The environmental persistency and potency of ^{90}Sr calls for urgent development of high-throughput tests to establish levels of exposure and to help triage potentially exposed individuals who were in the immediate area of the disaster. In response to these concerns, our team focused on developing a robust metabolomic profile for ^{90}Sr exposure in urine using a mouse model. The sensitivity of modern time-of-flight mass spectrometry (TOFMS) combined with the separation power of ultra performance liquid chromatography (UPLC) was used to determine perturbations in the urinary metabolome of mice exposed to ^{90}Sr. The recently developed statistical suite, MetaboLyzer, was used to explore the mass spectrometry data. The results indicated a significant change in the urinary abundances of metabolites pertaining to butanoate metabolism, vitamin B metabolism, glutamate and fatty acid oxidation. All of these pathways are either directly or indirectly connected to the central energy production pathway, the tricarboxylic acid (TCA) cycle. To our knowledge, this is the first *in vivo* metabolomics to evaluate the effects of exposure to ^{90}Sr using the easily accessible biofluid, urine.

INTRODUCTION

During a nuclear or a radiologic disaster, the population is exposed to different types of radiation through inhalation, external exposure and ingestion of contaminated food and water sources. In the case of a nuclear bomb explosion or damage to a nuclear reactor core such as in the Chernobyl and Fukushima accidents, radionuclides are released into the environment. The most feared and environmentally persistent radionuclides are Cesium-137 (^{137}Cs) and Strontium-90 (^{90}Sr). The effects of exposure to ^{137}Cs in serum and urine are the topic of a previous metabolomic study in mice, in which we established a metabolomic signature for exposure to ^{137}Cs in serum and urine (*1*). In continuation of our efforts to develop unique metabolomic signatures for exposure to internal emitters, the current study explored the biological effects following exposure to ^{90}Sr in mice using a similar metabolomics workflow.

Strontium-90, like ^{137}Cs, is a fission product of uranium and plutonium with a half-life of 28.8 years. Although ^{90}Sr is less likely to be released after a nuclear event and is less volatile than ^{137}Cs, it still poses a serious health risk. The most common source of ^{90}Sr exposure is through consumption of contaminated food and water after an event. Being a Group II element in the periodic table, ^{90}Sr has biochemical properties similar to calcium and after ingestion it can become incorporated into bone and bone marrow. Thus, ^{90}Sr is considered a ''bone seeker'', which can result in bone cancer, leukemia and cancers associated with the surrounding soft tissue. ^{90}Sr decays by beta emission into Yttrium-90, another beta emitter, which can further contribute to the radiation dose in bone and surrounding tissue (*2*). Due to the health effects associated with ^{90}Sr, it is important to identify the primary cellular targets of ^{90}Sr and determine a robust signature of exposure in easily obtainable biofluids to quickly and accurately triage patients while still in the field after a radiological disaster.

In the current study, we focused on determining a urinary metabolomic signature in mice after exposure to ^{90}Sr at different time points, and cumulative doses over the course of 30 days via ultra-performance liquid chromatography coupled with mass spectrometry (UPLCMS). The sensitivity and accuracy of UPLCMS combined with our powerful statistical software allowed for the detection of subtle changes in the urinary metabolomic profile. The measured

Editor's note. The online version of this article (DOI: 10.1667/RR14011.1) contains supplementary information that is available to all authorized users.

[1] Address for correspondence: Georgetown University, Biochemistry and Molecular and Cellular Biology, 3970 Reservoir Rd, NW, New Research Building E504, Washington D.C. 20057; e-mail: mg668@georgetown.edu.

TABLE 1
Dose Coefficient for $^{90}Sr + {}^{90}Y$ for Each Time Period (Gy.Bq^{-1} of Administered Activity)

Duration of study (days)	Dose coefficient (Gy.Bq^{-1})
7	8.79×10^{-6}
9	1.07×10^{-5}
25	2.34×10^{-5}
30	2.68×10^{-5}

absorbed doses to the skeleton ranged from 1.2–5.2 Gy over 30 days. The initial dose rate in this study was at 0.21 mGy/min while by the end of the experiment the dose rate had dropped to 0.12 mGy/min. The effects of changes in dose rate on the measured end points, although well recognized by the authors, could not be addressed in this study, since it is not possible to determine the effects of dose, dose rate and decreasing dose rate in a single study. More importantly, as in the case with ^{137}Cs, this radiation model continues to irradiate the cells at risk during the entire experimental period, compared to a relatively instantaneous dose delivery from an external radiation source such as X rays. The goal of this study was to establish a robust metabolomic response to ^{90}Sr in urine of mice and compare the results to known markers of external beam gamma irradiation and ^{137}Cs exposure.

MATERIALS AND METHODS

Debrisoquine sulfate, 4-nitrobenzoic acid (4-NBA) and UPLC-grade solvents such as acetonitrile, water and isopropanol were purchased from Fisher Scientific (Hanover Park, IL). 4-Guanidinobutyric acid, riboflavin, retinoic acid, (−)-epinephrine, hippuric acid, nicotinic acid, S-(5′-adenosyl)-L-homocysteine, taurine, uric acid, homovanillic acid, acetylcarnitine and carnitine were purchased from Sigma-Aldrich®, (St. Louis, MO). The METLIN (*3*) database (La Jolla, CA) was used for tandem MS (MS/MS) validations of 4-aminobutanoate, 3-hydroxybutanoate and quinolinic acid.

Animal Irradiation and Sample Collection

This study was conducted in accordance with applicable federal and state guidelines and was approved by the Institutional Animal Care and Use Committee of the Lovelace Biomedical and Environmental Research Institute (LBERI). C57Bl/6 mice (approximately 10–12 weeks old, 25–30 g) were received from Charles River Laboratories (Frederick, MD) and were quarantined for 14 days prior to group assignment by body weight stratification for randomization onto the study.

Animals were administered ^{90}Sr intravenously by tail vein injection with 200 ± 0.3 kBq $^{85/90}SrCl_2$ solution in a volume of 50 μL. Strontium-85 (^{85}Sr) was used as a tracer for measuring strontium whole-body content. Strontium-85 comprised approximately 1% of the total strontium activity. After $^{85}Sr/^{90}Sr$ administration, mice were housed individually in microisolator cages with lead shielding to prevent radiation exposure by cross irradiation from adjacent mice that were sources of radiation. All animals had unlimited access to Teklad Certified Global Rodent Diet 2016 (Harlan® Laboratories Inc., Madison, WI) and water except during dose administration and whole-body *in vivo* counting. No adverse effects were noted on the animals during the course of the study.

On scheduled necropsy days (4, 7, 9, 25 and 30 days after $^{85}Sr/^{90}Sr$ administration), animals were euthanized by intraperitoneal injection of Euthasol® [>150 mg/kg (390 mg/mL pentobarbital and 50 mg/mL phenytoin in sterile saline)] and weighed. Whole blood was collected by cardiac puncture in a sterile hood. When recoverable volumes were available, urine was collected directly from the bladder with a needle and syringe.

TABLE 2
Committed Absorbed Dose to Skeleton Doses for Each Time Period

Duration of study (days)	Committed absorbed dose to skeleton (Gy)
7	1.81
9	2.12
25	4.76
30	5.25

Dosimetry of ^{90}Sr in Mice

Animals were measured for $^{85}Sr/^{90}Sr$ whole-body content using the LBERI *in vivo* photon counting system described previously (*4*). Animals were placed in small containers with breathing holes, and daily measurements were taken to determine the amount of radioactivity present in each animal on days 0–7, then on day 9, 12, 16, 20, 25, 27 and 30 after $^{85}Sr/^{90}Sr$ administration (until the time of necropsy). The measurement system was calibrated for different geometries; phantoms representing the animal body and biological samples were developed using a $^{85/90}Sr$ NIST-traceable standard solution. Calibration was performed each day prior to measurement, and animals and samples were measured for 3 min.

The ^{90}Sr whole-body retention profile was derived from whole-body measurements. The whole-body retention data from each mouse was fitted individually to negative exponential functions. The average values of the parameters of the whole-body retention equation are shown in Eq. (1),

$$R_{(t)} = 52.1e^{-2.0t} + 20.7e^{-0.13t} + 27.2e^{-0.0049t} \quad (1)$$

where $R_{(t)}$ represents the whole-body ^{90}Sr content at time [(t) in days] expressed as percentage of the injected ^{90}Sr activity. The biological half-times were 0.3, 5.3 and 139 days, respectively.

To calculate the committed absorbed dose to the skeleton, the dose coefficient (Gy.Bq^{-1} of administered activity) was derived using Eq. (2). The comparison between the whole-body activity and the ^{90}Sr content in the skeleton at sacrifice time shows that about 95% of the whole-body activity was located in the skeleton for all time periods. Thus, the retention parameters of Eq. (1) were used to calculate the total number of nuclear transformations (Bq s) in the skeleton for each time period of the study. The S value (Gy/Bq s) used in Eq. (2) was derived specifically for young adult mice and rats by Stabin *et al*. (*5*). The dose coefficients (Gy Bq^{-1} of administered activity) for the various time periods used in this study are shown in Table 1.

The committed absorbed doses to the skeleton for each animal were calculated by multiplying the dose coefficient (Gy Bq^{-1}) related to the specific sacrifice time for each animal in the study by the administered activity (Bq). The average committed absorbed doses to the skeleton for each time period are shown in Table 2.

$$\frac{D_T}{A} = \int_{t_0}^{t_0+t} \tilde{A}(s) \times S(r_T \leftarrow r_S, t)\left(\frac{Gy}{Bq}\right), \quad (2)$$

where: $\tilde{A}(s)$ is the time-integrated activity (Bq s), equal to the total number of nuclear transformations in the source region (skeleton); $S(r_T \leftarrow r_S, t)$, in Gy per Bq s, is the S value from r_S to r_T of $^{90}Sr + {}^{90}Y$, where the S value for a given source (r_S)-target (r_T) pair is the mean absorbed dose to the target organ per $^{90}Sr + {}^{90}Y$ total number of nuclear transformations in the source region.

TABLE 3
Average Cumulative Doses for Each Study Group (Gy) and the Time of Necropsy is Listed in Days after ^{90}Sr Exposure

Study group	Necropsy (days after exposure)	Number of mice per study group	Internal dose (skeleton dose, Gy)	Creatinine (μM)
Control	7, 9	9	NA	1.3 ± 0.091
Control	25, 30	4	NA	1.4 ± 0.099
^{90}Sr exposed	7, 9	7	2.0 ± 0.28	1.2 ± 0.069
^{90}Sr exposed	25, 30	6	5.0 ± 0.62	1.2 ± 0.077

Note. The average levels of creatinine in urine for each study group are listed in terms of concentration (μM).

Sample Preparation and Mass Spectrometry Analysis

Urine samples were prepared by diluting each sample 1:4 in a 50% acetonitrile solution containing the internal standards, 30 μM of 4-nitrobenzoic acid and 2 μM of debrisoquine. The samples were centrifuged at 18,000 rcf to precipitate out the proteins. A 5 µL aliquot of the recovered supernatant was then injected into a reverse-phase 50 × 2.1 mm ACQUITY® 1.7 µm C18 column (Waters® Corp., Milford, MA) coupled to a time-of-flight mass spectrometry (TOFMS). The 13 min long mobile phase gradient started with aqueous solvent (98% water: 2% acetonitrile with 0.1% formic acid) and switched to 100% organic (acetonitrile) at a flow rate of 0.5 mL/min. The Q-TOF Premier™ (Waters Corp.) mass spectrometer was operated in positive (ESI^+) and negative (ESI^-) electrospray ionization modes. The acquired centroid mass spectrometer data was then processed using MassLynx™ software (Waters Corp.). Furthermore, twofold dilutions were performed using the internal standards at the initial concentration of 150 µg/mL to the final concentration of 0.59 µg/mL. The internal standards were also spiked into pooled control urine samples and processed every 7 injection intervals. The calculated standard curve for each internal standard was used to determine the relative abundance of different metabolites in each ionization mode.

Statistical Analysis

As described in our previous study (*6*) MarkerLynx™ software (Waters Corp.) was used to extract spectral features from raw chromatograms into a data matrix consisting of the retention time, mass-to-charge ratio (*m/z*) and abundance value for each ion. To determine the peak areas of internal standards, QuanLynx™ (Waters Corp.) was used. RandomForest was then used, initially to explore the overall urinary metabolomic signatures of the two dose/time points compared to that of the control mice. Subsequently, MetaboLyzer was used for in-depth statistical analysis of the data and for assigning putative identities to each ion (*7*). As described in our previous studies (*4*), MetaboLyzer was used to select ions that were present in at least 70% of the samples in all study groups with nonzero abundance values (complete-presence ions). The data were then log transformed and analyzed using the nonparametric Mann-Whitney U test for statistical significance ($P < 0.05$). The log transformed statistically significant complete-presence ion data were further utilized for principal component analysis (PCA) via singular value decomposition for the purpose of data visualization. Statistical significance testing for ions with nonzero abundance values in at least 70% of the samples in only one group (referred to as partial-presence ions) were analyzed as categorical variables for presence status (i.e., nonzero abundance) via Fisher's exact test ($P < 0.05$).

Metabolic Pathway Analysis

The putative identities of all statistically significant ions (both complete- and partial-presence) were used for pathway mapping in MetaboLyzer via the Human Metabolome Database (HMDB), LipidMaps and the Kyoto Encyclopedia of Genes and Genomes (KEGG) database (*8*). The maximum *m/z* tolerance was set at 20 parts per million (ppm), while accounting for possible adducts, H^+, Na^+ and/or NH_4^+ in the ESI^+ mode, and H^- and Cl^- in the ESI^- mode. The KEGG annotated pathways associated with these putative metabolites were also identified. Later, tandem mass spectrometry was used to generate fragmentation patterns for the metabolites of interest. These MS/MS fragmentations were then compared against those of matching pure chemicals or published MS/MS spectra on METLIN (*3, 9*) and HMDB for validation purposes.

RESULTS

RandomForest was initially used to assess the overall urinary metabolomic signatures of mice 7 and 9 days after ^{90}Sr exposure (average cumulative dose of 2.0 Gy), and 25 and 30 days after ^{90}Sr exposure (average cumulative dose of 5.0 Gy) compared to control mice. Supplementary Fig. S1A (http://dx.doi.org/10.1667/RR14011.1.S1) shows that the overall metabolomic signature of the ^{90}Sr-exposed mice from both time point groups are distinctly separate from that of control mice based on the normalized urinary levels of 25 most variable ions. While the urinary metabolomic profile of the exposed mice is clearly separate from the controls, the heatmap in Supplementary Fig. S1B (http://dx.doi.org/10.1667/RR14011.1.S1) shows a persistent decrease in the levels of 64 highest ranked variable ions across the two dose/time points (ESI^+ mode data). Additional in-depth statistical analyses were performed with the MetaboLyzer, which was employed to determine the statistical significance of individual ions (Mann-Whitney, $P < 0.05$) and their putative identity and pathway associations in both ESI modes.

At necropsy, urine could not be collected from the bladder of some of the mice at several time points due to the mice completely evacuating their bladders while still in their home cages. To increase the statistical power during analysis, we combined the results obtained from urine samples collected at day 7 and 9 after exposure, and averaged the skeletal doses. The average skeletal dose for these samples was 2.0 ± 0.28 Gy and the total number of samples in this dose group was 7, with 9 samples in the control group. The same approach was taken towards the urine samples collected at day 25 and 30 after exposure with the average dose of 5.0 ± 0.62 Gy. In addition all the available control samples were grouped for the statistical analyses in MetaboLyzer. Table 3 summarizes the number of samples per each dose and time point group and the matched controls. This table also contains the relative concentration of creatinine in each study group. The levels

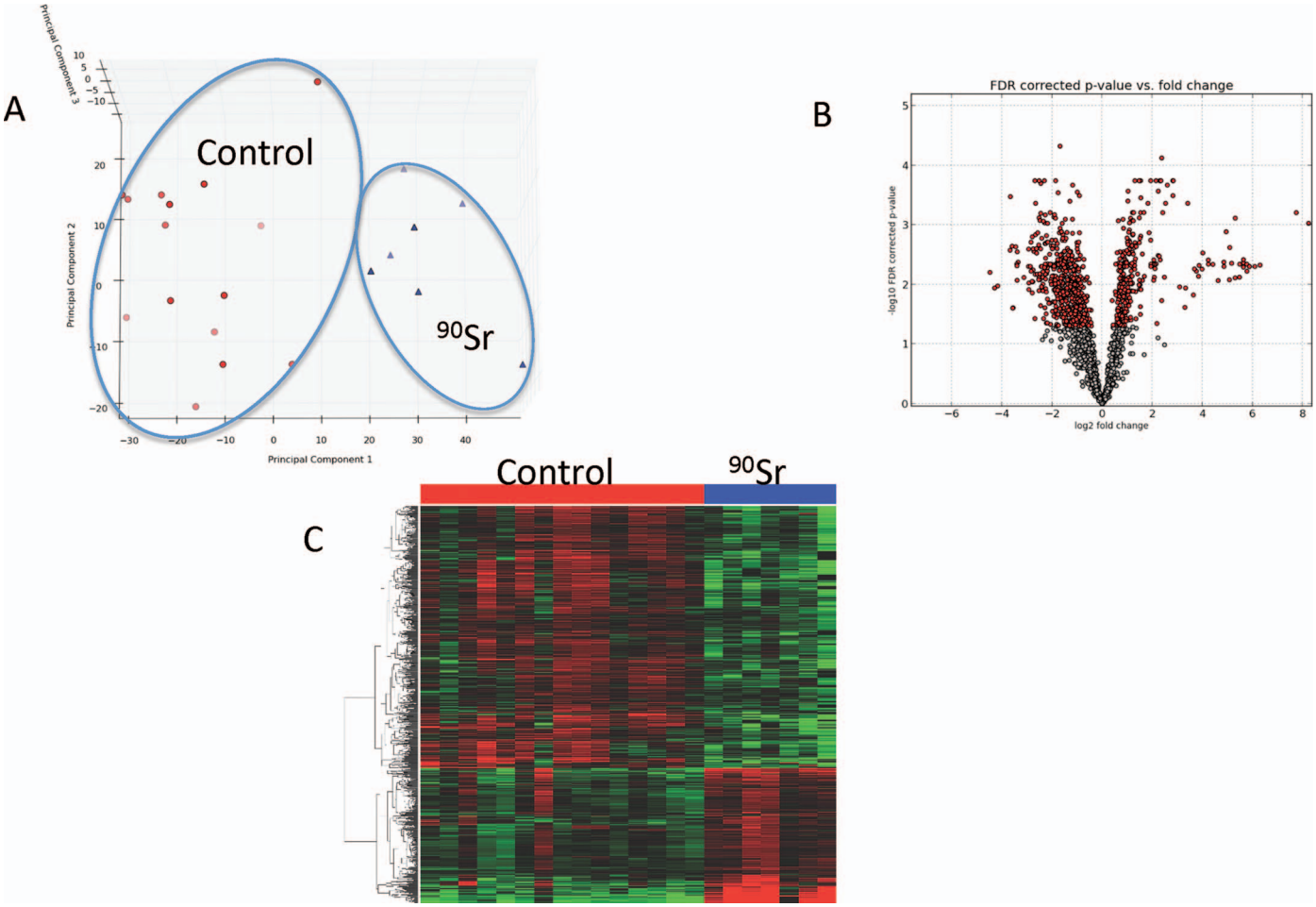

FIG. 1. Panel A: The overall metabolomic signature of urine from mice after exposure to ^{90}Sr after day 7 and 9 at average cumulative dose of 2.0 Gy is clearly distinguishable from that of the control mice as shown in this principal component analysis (PCA) created in MetaboLyzer. Panel B: The volcano plot generated in MetaboLyzer depicts in red the ions that show statistically significant perturbations (Mann-Whitney U test, $P < 0.05$) in their urinary excretion levels 7 and 9 days after exposure to ^{90}Sr. The positive scale on the x axis (log2 fold change) of this volcano plot refers to an increase while the negative scale refers to a decrease in the urinary excretion of ions after exposure. The y axis on this plot displays the FDR corrected significance of the perturbations in the urinary levels of ions after exposure. Panel C: The heatmap generated in MetaboLyzer shows a panel of ions whose urinary excretion levels change most significantly at day 7 and 9 after ^{90}Sr exposure. Two-thirds of the plot shows ions with decreased (green) urinary levels after ^{90}Sr exposure, and the bottom one-third of the plot shows ions with increased (red) levels after ^{90}Sr exposure at day 7 and 9.

of creatinine remained relatively unchanged throughout the study for the control and the exposed groups. We therefore normalized the abundance values of each ion to creatinine in our data matrix. The normalized data was then used in MetaboLyzer to establish a unique urinary metabolomic profile for exposure by ^{90}Sr at each of the doses/time points with respect to the control urine samples.

The principal component analysis plot in Fig. 1A shows a clear separation between the overall metabolomic profiles of control and ^{90}Sr-exposed urine samples at day 7 and 9 after exposure. The same separation in urinary metabolomic profiles was observed at the average dose of 5.0 ± 0.62 Gy when compared to the controls (Fig. 2A). Figure 2B shows a volcano plot of the *P* value (−1*log10) versus the fold change (log2) for all the complete-presence urinary spectral features at the average dose of 2.0 ± 0.28 Gy, and highlights the most statistically significant changes in their urinary abundances after exposure (red circles).The red circles to the right of the zero on this axis are the statistically significant spectral features whose urinary abundances increase significantly after exposure, and to the left of the zero are those whose urinary abundances decreased significantly as a result of ^{90}Sr exposure. It is evident from this plot that more urinary ions showed a decrease in their abundances after exposure at an average skeletal dose of 2.0 ± 0.28 Gy. This is also evident from the heatmap in Fig. 1C, which shows the changes in the urinary abundance of the most statistically significant ions. Almost two-thirds of these ions show decreased urinary levels after exposure. This post-exposure decrease in urinary abundances of statistically significant ions is even more evident at the later time points at the average skeletal dose of 5.0 ± 0.62 Gy (Fig. 2B and C). Since the water consumption and the urine output, as well as the weight of the mice did not

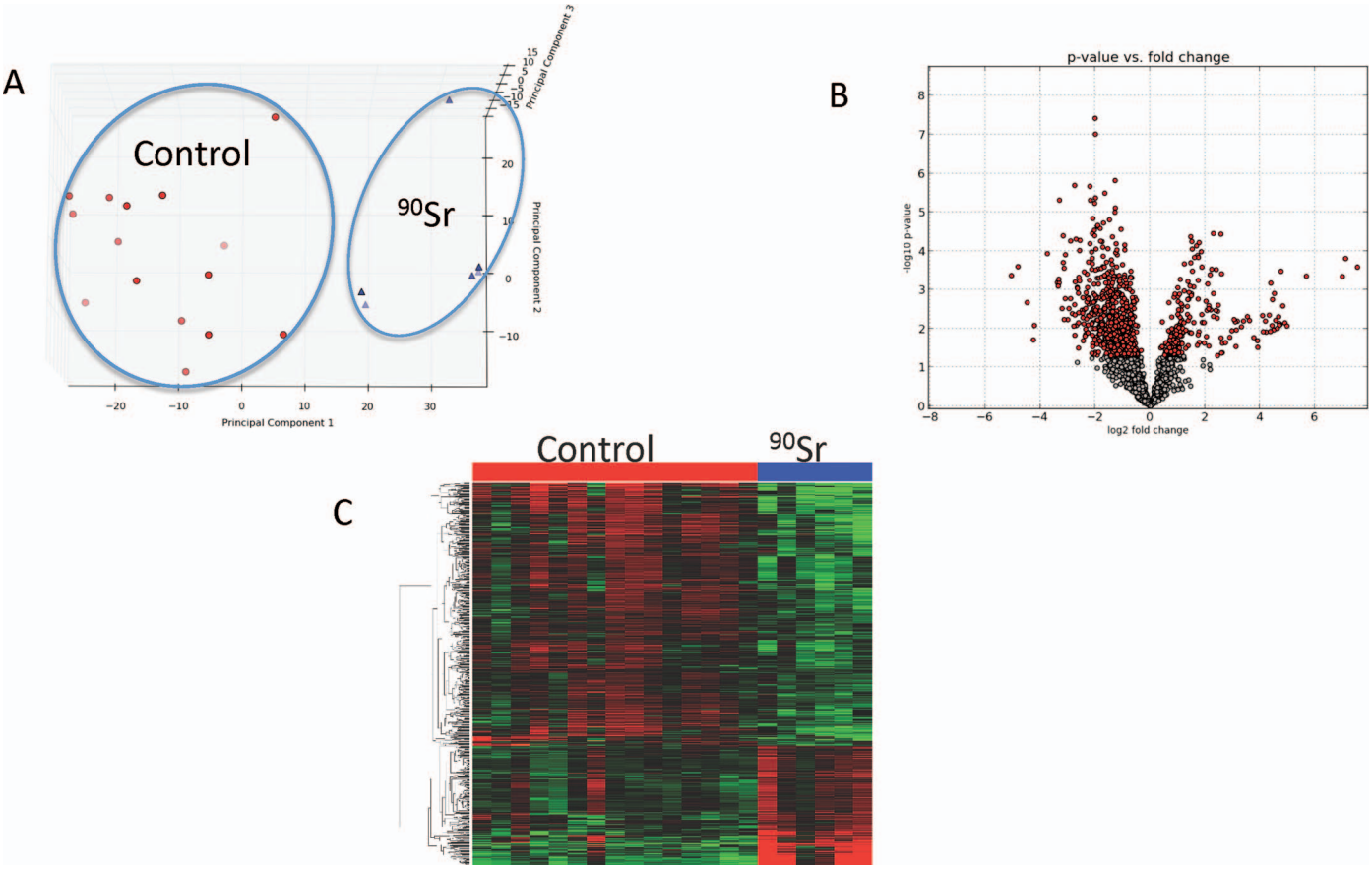

FIG. 2. Panel A: A clear separation is observed in this PCA of the overall metabolomic signature of urine from mice collected on day 25 and 30 after internal exposure to ^{90}Sr at the average cumulative dose of 5.0 Gy and that of urine from control mice. Panel B: The red dots in the MetaboLyzer-generated volcano plot represent ions that show statistically significant perturbations (Mann-Whitney U test, $P < 0.05$) in their urinary excretion levels after 25 and 30 days of exposure to ^{90}Sr. The number of ions on the negative scale of the x axis is larger than on the positive scale, which suggests that most of the statistically significant ions were found at lower levels in the urine ^{90}Sr-exposed mice compared to the controls. This is also evident from the heatmap in panel C, where almost three-quarters of the depicted ions show lower urinary levels in the ^{90}Sr-exposed mice than in the control mice.

change significantly throughout the course of the study, this observation may indicate perturbations in the metabolic pathways associated with these statistically significant urinary ions. Thus, the next phase of the study was focused on identifying individual urinary ions with significantly changed levels after exposure, and determining their association with various metabolic pathways.

We initially focused on urinary radiation exposure markers, which have been reported in the literature and our previous work with external gamma exposure and another internal emitter, Cesium-137 (*4, 6, 10, 11*). These urinary metabolite markers are listed in Table 4 along with the direction of change in their abundances after exposure to different types of radiation. We confirmed the identities of these markers in the urine samples studied here via MS/MS using authentic chemical standards. The relative abundances of these ions in the urine of mice exposed to ^{90}Sr at both average doses of 2.0 and 5.0 Gy were established using standard curves for each metabolite and shown as down arrows for decreased post-exposure urinary abundance, and up arrows for increased post-exposure urinary abundances. Xanthurenic acid, tiglylcarnitine and hexanoylcarnitine were detected at lower levels in urine of mice after exposure to ^{90}Sr, which is similar to what we observed in the urine of mice after exposure to ^{137}Cs and X rays at low dose rate (3 mGy/min) (*4, 10*). However, no changes were observed in the urinary excretion of these metabolites afer X irradiation at the high dose rate of 1 Gy/min. There are also no reports of attenuation in the urinary levels of these metabolites after 1 Gy gamma irradiation in the literature. Therefore, these metabolites may be specific to exposure to low dose rates from either an external beam source or an internal emitter such as ^{137}Cs or ^{90}Sr. The metabolites that have shown robust changes in their urinary excretion levels after exposure to internal emitters, low dose rate and high dose rate X and gamma irradiations are hippuric acid, citrate and uric acid. These metabolites may serve as general radiation exposure markers, while the former may serve as dose-rate specific markers.

Finally, we focused on determining the identities of urinary ions, which displayed the most statistically significant changes after internal exposure to ^{90}Sr. Among

TABLE 4
Robust Metabolite Markers Common among Different Exposure Types

			Change in urinary excretion				
	*m/z*_RT	Putative ID	GAMMA EXPOSURE (1 Gy) 24 h after exposure	High dose rate (1 Gy) (1 Gy/min) 48 h after exposure	Low dose rate (1 Gy) (3 mGy/min) 48 h after exposure	^{137}Cs exposure 1.95 Gy 48 h after exposure	^{90}Sr exposure 1.83 ± 0.17 Gy 7 days after exposure
1	206.045_1.5374	Xanthurenic acid	-	No change	↓	↓	↓
2	244.1547_2.0563	Tiglylcarnitine	-	↑	↓	↓	↓
3	260.1864_3.3971	Hexanoylcarnitine	-	↑	↓	↓	↓
4	180.0659_1.966	Tiglylglycine	-	↑	↑	↑	-
5	178.0517_1.9308	Hippuric acid	↑ (*11*)	↑	↑	↑	↑
6	158.0831_1.5708	Isovalerylglycine	↓ (*11*)	↓	↓	↓	-
7	191.0201_0.3574	Citrate	↓ (*6, 15*)	↓	↓	↓	↓
8	167.0215_0.326	Uric acid	↑ (*15, 16*)	↑	↑	↑	↑
9	145.0153_0.3143	α-ketoglutaric acid	↓ (*15*)	↓	↓	↓	-

these ions, we were able to confirm the identities of pantothenic acid and riboflavin via tandem mass spectrometry. The urinary levels of these vitamin B metabolites showed more than a threefold decrease after exposure at both 2.0 and 5.0 Gy as shown in Fig. 3 and Table 5. The levels of these two metabolites did not recover by the end of the experiment. Because there was no change in diet and food intake of the mice throughout the study, the decrease in the levels of these two metabolites are indicative of prolonged internal exposure to ^{90}Sr. Cofactors derived from

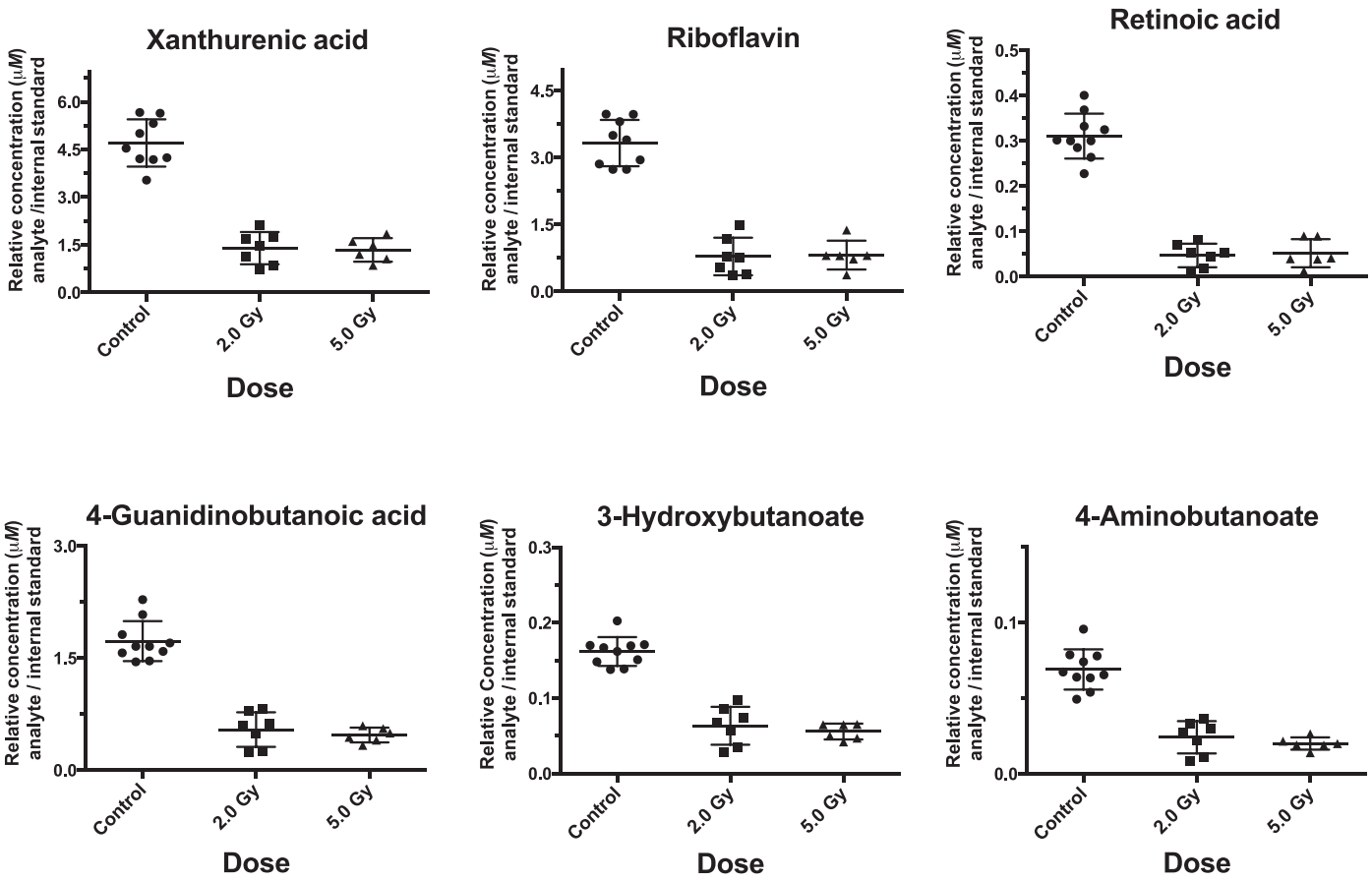

FIG. 3. Six selected urinary metabolite markers of exposure to ^{90}Sr, which follow similar decreasing trends after exposure. The decrease in the urinary excretion levels of these metabolites is seen as early as day 7 and 9 after exposure at the average skeleton dose of 2.0 Gy and lasts through the course of the 30 day study at the average dose of 5.1 Gy by day 25 and 30. The y axis on each figure shows the urinary levels of the metabolite with respect to an appropriate internal standard in the units of concentration (μ*M*) and the x axis specifies the dose point.

TABLE 5
Metabolites Showing Statistically Significant Decreases in their Urinary Excretion Levels after ^{90}Sr Exposure throughout the 30 Day Study

Name[a]	ESI mode	*m/z*_RT	Error (ppm)	Fold change[b]	
				2.0 ± 0.28 Gy 7, 9 days after ^{90}Sr	5.0 ± 0.62 Gy 25, 30 days after ^{90}Sr
Pantothenic acid	Positive	220.1190_1.6270	6.36	0.17	0.13
NA	Positive	202.0193_2.9741	NA	1.62	1.57
NA	Positive	369.1908_3.4312	NA	1.35	1.76
Indolelactic acid	Negative	204.0673_3.9967	7.72	0.67	0.69
Glutaconic acid	Negative	129.0201_0.5645	9.65	0.40	0.52
Glutamate (Cl^- adduct)	Negative	182.0461_0.8448	5.21	0.66	0.65
Quinolinic acid	Negative	166.0182_0.3361	6.10	0.86	0.80
Malate (Cl^- adduct)	Negative	167.9827_0.3577	8.96	0.70	0.59
NA	Negative	339.1637_2.8520	NA	2.84	3.01
NA	Negative	128.9610_0.2692	NA	3.43	3.78

[a] Identities of ions with names were validated via MS/MS using METLIN and HMDB databases.
[b] Fold change was calculated by dividing the average peak area of ion at each dose group by that of a matched control group.

riboflavin (Fig. 3) and pantothenic acid (Table 5) are required for the conversion of pyruvate to acetyl-CoA as part of the energy production pathway. The resulting acetyl-CoA is then employed into adenosine triphosphate (ATP) production from the tricarboxylic acid (TCA) cycle. The decrease in the urinary levels of riboflavin and pantothenic acid is in line with a sharp decrease in the urinary excretion levels of TCA cycle intermediates, citrate and malate. In our previous study with internal exposure to ^{137}Cs, we observed similar decreases in urinary excretion of citrate after exposure, with levels returning to those of pre-exposure by the end of the study. However, in the case of ^{90}Sr exposure, the magnitude of attenuation in these two TCA cycle metabolites is greater and the levels do not recover to those of pre-exposure by the end of the 30-day period. Therefore, this persistent decrease in the urinary levels of ions appears to be unique to ^{90}Sr exposure with more than 75% of the statistically significant urinary ions showing similar decreasing levels after exposure.

Among the identified and statistically significant metabolites were two dicarboxylic acids, glutaconic acid and quinolinic acid (Table 5). Dicarboxylic acids are the result of fatty acid catabolism through ω oxidation. Therefore, dicarboxylic acids are part of the energy production pathway and changes in their urinary excretion may signal a shift in energy metabolism. The urinary excretion levels of these two dicarboxylic acids showed almost a twofold decrease after exposure throughout the course of the study. In addition, two intermediates in the tryptophan pathway metabolism, xanthurenic acid (Fig. 3) and indolelactic acid (Table 5) also showed significant decreases in their urinary excretion levels after exposure. The tryptophan pathway is also tied into the energy production machinery through acetyl-CoA. A decrease in its intermediates may result in a drop in the levels of free acetyl-CoA and slower energy production. Such decrease in the urinary excretion of metabolites associated with energy metabolism can point to a functional deficiency in mitochondria, which are the hub of energy production. Mitochondrial function and morphology are known to be affected under environmental stress and injury (*12*). Therefore, the results of this study along with our findings in our previous urinary metabolomics study of ^{137}Cs exposure highlight the involvement of mitochondrial pathways, such as TCA cycle and lipid metabolism, in response to radiation exposure.

Moreover, the results of this study identified significant perturbations in butanoate metabolism, yet another mitochondrial pathway. Butanoate metabolism is linked directly to the TCA cycle through succinate and indirectly through pyruvate and acetyl-CoA (Fig. 4). It is also associated with alanine, aspartate and glutamate metabolism, which is further associated with TCA cycle through glutamate. We found the urinary levels of glutamate and subsequently 4-hydroxybutanoate to be significantly lower after exposure. Butanoate metabolism, like the TCA cycle, is a mitochondrial metabolic pathway, which is important for energy production, cell proliferation and protection against inflammatory factors in colonocytes. It has been shown that butanoate deficiency in colonocytes can lead to energy deprivation and ultimately autophagy (*13*). The decrease in the levels of butanoate post ^{90}Sr exposure may signal a change in the energy production of colonocytes and a deficit in mitochondrial respiration. However, the majority of the dose was localized to the skeleton, so the target tissue for this drop in butanoate is uncertain. Interestingly, metabolites associated with butanoate metabolism were not found to be significantly perturbed in mice exposed to ^{137}Cs or those exposed to external gamma and X rays. While ^{137}Cs is primarily a gamma emitter, ^{137}Cs/^{137}Ba is also a beta-emitting radionuclide pair (1 beta per pair decay), so the unique ^{90}Sr response is not beta-ray specific.

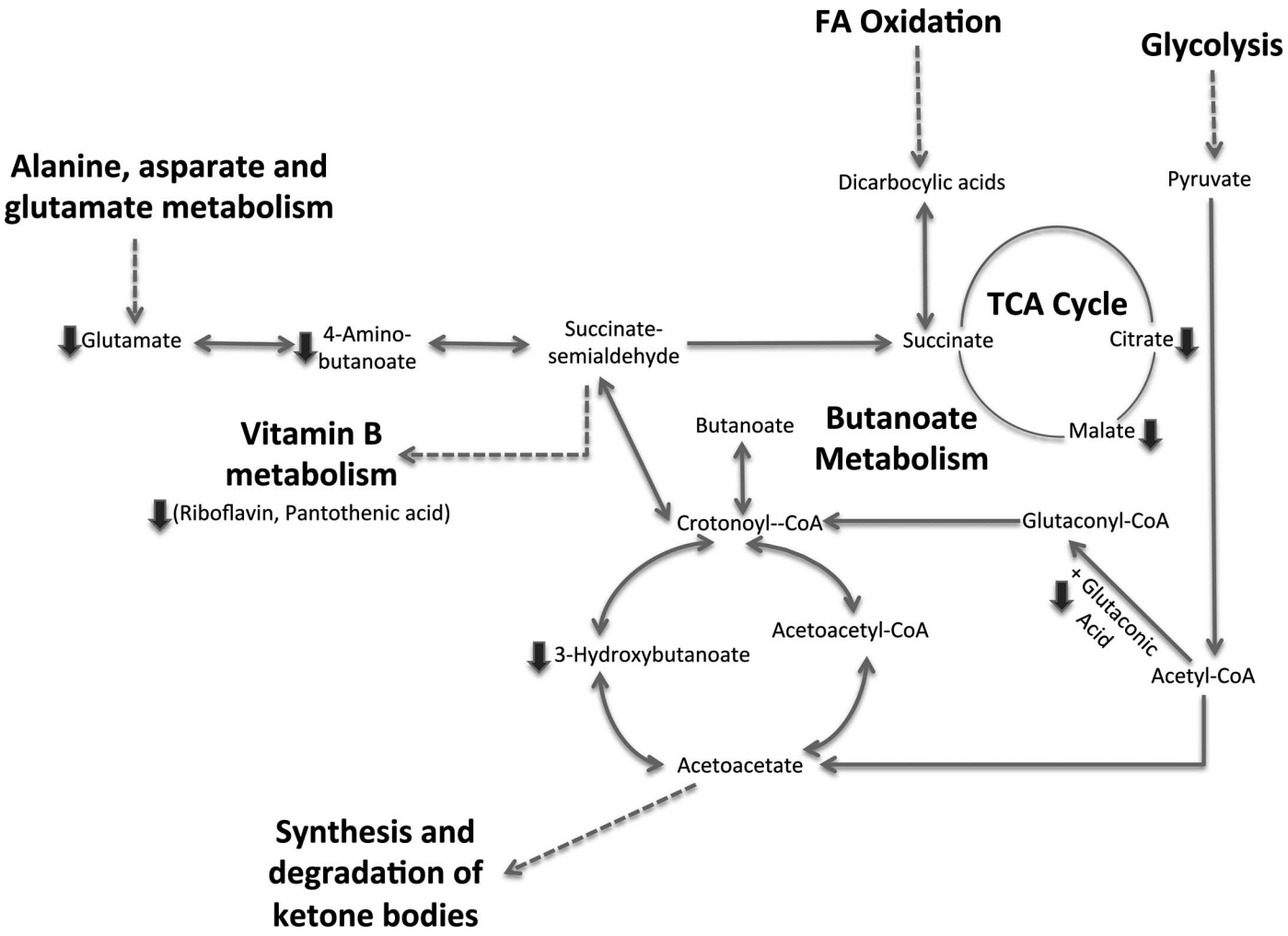

FIG. 4. This overall pathway elucidation is based on the association of individual validated and statistically significant metabolites with KEGG pathways. The butanoate metabolism is shown in the center as it was linked to TCA cycle, glycolysis, vitamin B metabolism and glutamate metabolism. These pathways are central to energy production. Intermediates of these pathways have been found at lower levels in the urine of ^{90}Sr-exposed mice at 2.0 Gy (day 7 and 9 after exposure) and 5.0 Gy (day 25 and 30 after exposure) compared to control mice.

DISCUSSION

In this study we investigated the effects of exposure to internal ^{90}Sr in mice through metabolomics. This study follows our earlier work on the effects of exposure to another internal emitter, ^{137}Cs (*4*). Both ^{137}Cs and ^{90}Sr irradiate the organs and tissues of the mouse for the duration of the study. However, the spatial distribution of dose is different for the two radionuclides. About 95% of ^{137}Cs decays by beta emission to ^{137m}Ba, which decays emitting photon energy of 662 keV. Because of the high-energy gamma irradiation associated with the cesium deposition in the skeletal muscle tissue, the dose distribution in the body is uniform. However, ^{90}Sr decays by beta emission to ^{90}Y, which also decays by beta emission. Therefore, ^{90}Sr + ^{90}Y can be considered as pure beta emitters, with most of the committed dose delivered to skeleton tissue and bone marrow. Thus, the aim of the current study was to identify a unique metabolomic signature for ^{90}Sr.

The urine from mice exposed to ^{90}Sr at two cumulative doses, 2.0 ± 0.28 Gy and 5.0 ± 0.62 Gy, was collected in the course of this 30 day study. The overall urinary metabolomic signature of the control mice was distinctly different from that of mice after 2.0 and 5.0 Gy exposure based on the top 25 variable ions as ranked by Random-Forest in Supplementary Fig. S1A (http://dx.doi.org/10.1667/RR14011.1.S1). Although the overall metabolomic signatures of the two dose/time points are also distinguishable, there is a persistent decrease in the urinary levels of the top ranked ions after exposure as shown in Supplementary Fig. S2B (http://dx.doi.org/10.1667/RR14011.1.S1). The results of this preliminary statistical analysis in Random-Forest showed attenuation in the levels of many metabolites after exposure, with a few metabolites showing an increase in their urinary excretion levels after exposure. This is also evident from subsequent dose-specific analysis in MetaboLyzer, as shown in the Fig. 1 volcano plot. These results are in contrast to what we observed in the urine of mice

exposed to ^{137}Cs. However, a closer look at individual urinary ions revealed that these two internal emitters affect the levels of several ions similarly. For instance, the levels of xanthurenic acid, tiglylcarnitine, hexanoylcarnitine, hippuric acid, citrate and uric acid showed similar perturbations after exposure to ^{90}Sr and ^{137}Cs (Table 4). These ions have also been reported in studies with external beam irradiation (Table 4). While these ions may be common to external beam irradiation and internal emitter exposure (^{137}Cs and ^{90}Sr), each radiation type produces a unique metabolomic signature, which may be used to determine the type of exposure in a biological sample. For example, ^{90}Sr exposure resulted in persistent attenuations in majority of the statistically significant ions, while ^{137}Cs exposure resulted in increases in more than half the detected urinary ions. The attenuation in the urinary levels of ions after ^{137}Cs exposure were dose specific and levels reverted back to those of pre-exposure by the end of the 30 day study (*4*). Therefore, the widespread persistent decreases in levels of urinary ions is unique to ^{90}Sr exposure.

Furthermore, pathway analysis of the statistically significant ions mapped 3-hydroxybutanoate, acetoacetate, and 4-aminobutanoate, to butanoate metabolism. The urinary levels of these metabolites decreased significantly after ^{90}Sr exposure. Butanoate metabolism is a mitochondrial pathway and is central to energy production in colonocytes. This pathway is crosslinked to TCA cycle, glycolysis, vitamin B metabolism, fatty acid oxidation, and glutamate metabolism (Fig. 4). We have identified at least two members of each of these pathways showing uniform significant decreases after ^{90}Sr exposure, which may be unique to exposure to beta-particle emission of ^{90}Sr. Furthermore, butanoate metabolism and TCA cycle are two important mitochondrial pathways involved in energy production. Therefore, any shift in the levels of metabolites associated with these pathways may signal a change in mitochondrial function and morphology.

Although ^{90}Sr is referred to as a ''bone seeker'' due to having similar physical and chemical properties as calcium, we were not able to find any markers of injury to bone or surrounding soft tissue in the urine of mice in this study. This is probably because leukemia and soft tissue injury have been shown to occur after long-term chronic exposure to higher doses of ^{90}Sr than those reported in this study (*14*).

CONCLUSION

In this study, we established a robust and unique metabolomic response to ^{90}Sr exposure in mice using urine, an easily accessible biofluid. Butanoate metabolism demonstrated the most significant perturbations in its associated metabolites. In addition, metabolites associated with TCA cycle, and vitamin B metabolism displayed significant changes in their urinary excretion levels. Although much work remains to establish a panel of field-deployable ^{90}Sr-exposure markers, butanoate metabolism appears to be a unique and promising target.

SUPPLEMENTARY INFORMATION

Fig. S1. The overall urinary metabolomic signature of mice exposed to ^{90}Sr at two average dose points (2.0 and 5.0 Gy) is clearly distinguishable from that of control mice.

Fig. S2. The overall metabolomic signatures of the two dose/time points are also distinguishable, there is a persistent decrease in the urinary levels of the top ranked ions after exposure

ACKNOWLEDGMENTS

This study was supported by the National Institutes of Health (National Institute of Allergy and Infectious Diseases), awarded to Dr. David J. Brenner (grant no. U19 A1067773) and the Proteomic and Metabolomics Shared Resources (grant no. P30 CA51008). The authors would like to thank Georgetown University's Radiation Safety Office, and Dr. Amrita Cheema and Kirandeep Gill at the Proteomic and Metabolomics Shared Resources for making the analysis of the radioactive specimens possible.

Received: December 29, 2014; accepted: March 19, 2015; published online: May 26, 2015

REFERENCES

1. Goudarzi M, Weber WM, Mak TD, Chung J, Doyle-Eisele M, Melo DR, et al. Metabolomic and lipidomic analysis of serum from mice exposed to an internal emitter, Cesium-137, using a shotgun LC-MS approach. J Proteome Res 2015; 14:374–94.
2. Raabe OG. Concerning the health effects of internally deposited radionuclides. Health Phys 2010; 98:515–36.
3. Smith CA, O'Maille G, Want EJ, Qin C, Trauger SA, Brandon TR, et al. METLIN: a metabolite mass spectral database. Ther Drug Monit 2005; 27:747–51.
4. Goudarzi M, Weber WM, Mak TD, Chung J, Doyle-Eisele M, Melo DR, et al. Development of urinary biomarkers for internal exposure by cesium-137 using a metabolomics approach in mice. Radiat Res 2014; 181:54–64.
5. Stabin MG, Peterson TE, Holburn GE, Emmons MA. Voxel-based mouse and rat models for internal dose calculations. J Nucl Med 2006; 47:655–9.
6. Tyburski JB, Patterson AD, Krausz KW, Slavik J, Fornace Jr AJ, Gonzalez FJ, et al. Radiation metabolomics. 1. Identification of minimally invasive urine biomarkers for gamma-radiation exposure in mice. Radiat Res 2008; 170:1–14.
7. Mak TD, Laiakis EC, Goudarzi M, Fornace Jr AJ. MetaboLyzer: a novel statistical workflow for analyzing Postprocessed LC-MS metabolomics data. Anal Chem 2014; 86:506–13.
8. Kanehisa M, Goto S. KEGG: Kyoto encyclopedia of genes and genomes. Nucleic Acids Res. 2000; 28:27–30.
9. Zhu ZJ, Schultz AW, Wang J, Johnson CH, Yannone SM, Patti GJ, et al. Liquid chromatography quadrupole time-of-flight mass spectrometry characterization of metabolites guided by the METLIN database. Nat Protoc 2013; 8:451–60.
10. Goudarzi M, Mak TD, Chen C, Smilenov LB, Brenner DJ, Fornace Jr AJ. The effect of low dose rate on metabolomic response to radiation in mice. Radiat Environ Biophys 2014; 53:645–57.
11. Johnson CH, Patterson AD, Krausz KW, Lanz C, Kang DW, Luecke H. Radiation metabolomics. 4. UPLC-ESI-QTOFMS-based metabolomics for urinary biomarker discovery in gamma-irradiated rats. Radiat Res 2011; 175:473–84.

12. Otera H, Mihara K. Mitochondrial dynamics: functional link with apoptosis. Int J Cell Biol 2012; 821676.

13. Donohoe DR, Garge N, Zhang X, Sun W, O'Connell TM, Bunger MK, et al. The microbiome and butyrate regulate energy metabolism and autophagy in the mammalian colon. Cell Metab 2011; 13:517–26.

14. Dungworth DL, Goldman M, Switzer J, McKelvie DH. Development of a myeloproliferative disorder in beagles continuously exposed to ^{90}Sr. Blood 1969; 34:610–32.

15. Lanz C, Patterson AD, Slavik J, Krausz KW, Ledermann M, Gonzalez FJ, et al. Radiation metabolomics. 3. Biomarker discovery in the urine of gamma-irradiated rats using a simplified metabolomics protocol of gas chromatography-mass spectrometry combined with random forests machine learning algorithm. Radiat Res 2009; 172:198–212.

16. Laiakis EC, Hyduke DR, Fornace Jr. AJ. Comparison of mouse urinary metabolomics profiles after exposure to the inflammatory stressors gamma radiation and lipopolysaccharide. Radiat Res 2012; 177:187–99.